



An Adult *Drosophila* Glioma Model for Studying Pathometabolic Pathways of Gliomagenesis

Kuan-Cheng Chi¹ · Wen-Chiuan Tsai² · Chia-Lin Wu^{3,4} · Tzu-Yang Lin^{5,6} · Dueng-Yuan Hueng^{1,7,8,9} 

Received: 28 August 2018 / Accepted: 11 October 2018 / Published online: 24 October 2018
© Springer Science+Business Media, LLC, part of Springer Nature 2018

Abstract

Glioblastoma multiforme (GBM), the most prevalent brain tumor in adults, has extremely poor prognosis. Frequent genetic alterations that activate epidermal growth factor receptor (EGFR) and phosphatidylinositol-3 kinase (PI3K) signaling, as well as metabolic remodeling, have been associated with gliomagenesis. To establish a whole-animal approach that can be used to readily identify individual pathometabolic signaling factors, we induced glioma formation in the adult *Drosophila* brain by activating the EGFR-PI3K pathway. Glioma-induced animals showed significantly enlarged brain volume, early locomotor abnormalities, memory deficits, and a shorter lifespan. Combining bioinformatics analysis and glial-specific gene knockdown in the adult fly glioma model, we identified four evolutionarily conserved metabolic genes, including *ALDOA*, *ACAT1*, *ELOVL6*, and *LOX*, that were involved in gliomagenesis. Silencing of *ACAT1*, which controls cholesterol homeostasis, reduced brain enlargement and increased the lifespan of the glioma-bearing flies. In GBM patients, *ACAT1* is overexpressed and correlates with poor survival outcomes. Moreover, pharmacological inhibition of *ACAT1* in human glioma cell lines revealed that it is essential for tumor proliferation. Collectively, these results imply that *ACAT1* is a potential therapeutic target, and cholesterol homeostasis is strongly related to glioma formation. This in vivo model provides several rapid and robust phenotypic readouts, allowing determination of the pathometabolic pathways involved in gliomagenesis, as well as providing valuable information for novel therapeutic strategies.

Keywords Glioma · Metabolism · *Drosophila* · *ACAT1*

Introduction

Glioblastoma multiforme (GBM), the most common primary malignant brain tumor, is highly proliferative, with extensive infiltration, poor prognosis, and resistance to standard

chemotherapies. The average survival for GBM patients is approximately 12 to 16 months after diagnosis [1, 2]. Even with standard treatment using maximal surgical resection followed by focal radiotherapy with concomitant and adjuvant chemotherapy, survival rates of GBM patients remain poor. Therefore,

Electronic supplementary material The online version of this article (<https://doi.org/10.1007/s12035-018-1392-2>) contains supplementary material, which is available to authorized users.

✉ Tzu-Yang Lin
tzuyanglin@gate.sinica.edu.tw

✉ Dueng-Yuan Hueng
hondy2195@gmail.com

¹ Graduate Institute of Medical Sciences, National Defense Medical Center, Taipei 114, Taiwan

² Department of Pathology, Tri-Service General Hospital, National Defense Medical Center, Taipei 114, Taiwan

³ Department of Biochemistry and Graduate Institute of Biomedical Sciences, College of Medicine, Chang Gung University, Taoyuan 33302, Taiwan

⁴ Department of Neurology, Chang Gung Memorial Hospital, Linkou 33305, Taiwan

⁵ Graduate Institute of Life Sciences, National Defense Medical Center, Taipei 114, Taiwan

⁶ Institute of Cellular and Organismic Biology, Academia Sinica, Taipei 11529, Taiwan

⁷ Department of Biochemistry, National Defense Medical Center, Taipei 114, Taiwan

⁸ Department of Biology and Anatomy, National Defense Medical Center, Taipei 114, Taiwan

⁹ Department of Neurological Surgery, Tri-Service General Hospital, National Defense Medical Center, Taipei 114, Taiwan

there is an urgent need to develop more effective therapeutic agents against GBM. To facilitate research in this field, appropriate preclinical glioma models are required for elucidating the genetic and molecular mechanisms underlying gliomagenesis and the development of novel treatment strategies.

Several animal models have been developed for modeling human glioma, including transgenic and xenograft-based murine, zebrafish, and fruit fly (*Drosophila*) models [3]. Noticeably, genetically engineered mouse models (GEMMs) have many advantages over other models (such as immunocompetent setting, tumor microenvironment, and intact blood–brain barrier). However, as generation of GEMM of glioma is a slow process due to long tumor latency, drug screening in these models is time-consuming and costly. In contrast, the fruit fly model is inexpensive but still has strengths such as the brain microenvironment [3]. Moreover, numerous gliomagenic pathways, such as the receptor tyrosine kinase (RTK) signaling and metabolic pathways, are highly conserved between fruit fly and humans. These features make *Drosophila* a valid and attractive model of human glioma. Furthermore, the short tumor latency (within weeks) and highly versatile genetic tools of the fly glioma model will facilitate rapid elucidation of the molecular pathways that drive gliomagenesis in vivo [4].

Metabolic rewiring is a crucial step in the transition from non-neoplasm to neoplasm. Glioma is no exception. Since Nobel Laureate Otto Warburg first proposed a metabolic adaptation in cancer cells [5], accumulating evidence indicates that metabolic signal transduction pathways, including those of glucose, glutamine, fatty acids, nucleotide, and extracellular matrix (ECM), are involved in facilitating tumorigenesis [6–8]. In glioblastoma, aerobic glycolysis and lipid metabolism contribute to the energy production associated with cell survival. The large databases Cancer Genome Atlas (TCGA) and REpository for Molecular BRAin Neoplasia DaTa (REMBRANDT) provide comprehensive records of the genomic and transcriptomic abnormalities driving gliomagenesis and have revealed core pathways, including the RTK/RAS/PI3K, p53, and Rb pathways [9–11]. Accumulating evidence shows that RTK pathway aberration is a key factor leading to metabolic reprogramming. Therefore, targeting key RTK downstream metabolic regulators might be an effective therapeutic strategy for malignant gliomas [12, 13]. The importance of metabolic processes has been demonstrated not only in gliomas but also in normal glia [14–16]. A recent global in vivo RNAi screen (6930 genes) in adult *Drosophila* for the effects on glial functions revealed that metabolic processes such as carbohydrate and lipid metabolism were highly represented and appeared to be essential in glia [16]. Novel approaches that target essential metabolic pathways in glia could become promising strategies for the treatment of gliomas, but only limited studies have been conducted to date.

Previously, a *Drosophila* larval glioma model was generated by coactivation of EGFR-Ras and PI3K as early as

embryogenesis in glial progenitor cells. This fly larval model recapitulates many key features of human GBM with regard to increased proliferation, migration, and invasiveness [17]. This larval model has been used to perform genetic screenings and identify new genes involved in glioblastoma development [18–20]. However, early activation of gliomagenic signaling pathways results in larval lethality, which does not recapitulate the characteristic symptoms of human GBM, especially in aspects related to adult patient survival and neurobehavioral problems. Since GBM is often diagnosed in the elderly population, with a median age over 62 years [21], an adult fly model that excludes developmental factors is more relevant to clinical situations. To achieve this, we modified the previous model by further introducing a temporal expression system [22]. This allowed us to induce glioma formation in the adult stage by simply altering the rearing temperature.

In this study, we utilized an EGFR-PI3K adult fly glioma model to investigate the genetic and molecular basis of gliomagenesis. Using candidate selection by combined bioinformatics analysis and analysis of essential metabolic genes of glia, we identified four genes, i.e., aldolase A (*ALDOA*), acyl-CoA:cholesterol acyltransferase 1 (*ACAT1*), elongation of very long chain fatty acids protein 6 (*ELOVL6*), and lysyl oxidase (*LOX*), whose expression level is associated with reduced patient survival. Glial-specific RNAi-mediated knockdown of *ALDOA*, *ACAT1*, *ELOVL6*, and *LOX* in the adult *Drosophila* glioma model suppressed gliomagenesis. Furthermore, pharmacological inhibition of *ACAT1* in human glioma cell lines significantly suppressed cancer cell proliferation. These results indicated that *ACAT1* can be an oncogenic biomarker in human high-grade gliomas. Furthermore, our new adult fly glioma model provides a useful in vivo tool for verification of potential GBM biomarkers.

Materials and Methods

In Silico Analyses

We used online database REpository for Molecular BRAin Neoplasia DaTa (REMBRANDT) from Project Betastasis (<http://betastasis.com/glioma/rembrandt/>) to determine Kaplan–Meier curves of patient survival based on *ALDOA*, *ACAT1*, *ELOVL6*, and *LOX* transcript levels as described previously [23]. Threshold was set at median expression for the respective *ALDOA*, *ACAT1*, *ELOVL6*, and *LOX* transcript.

Fly Strains

All stocks were maintained and conducted at ~23–25 °C and were provided with standard cornmeal–agar–yeast food. We established all genotypes by exploiting standard genetics. Fly stocks and all *UAS*-RNAi lines were obtained from the

Bloomington, VDRC, and NIG stock centers. Glioma fly brain phenotypes were assessed and imaged by Zeiss LSM880 confocal microscopy to visualize GFP-labeled signal in glia cells. Genotypes of transgenic flies were used in this study: *UAS-dp110^{CAAX}*, *UAS-dEGFR^Δ*; *UAS-hCD4-tdGFP*; *repo-GAL4, tub-GAL80^{ts}* for glioma flies and *UAS-hCD4-tdGFP*; *repo-GAL4, tub-GAL80^{ts}* for control flies. The detailed genotypes of flies used in this work are listed in supplemental Table 1.

Longevity Assay

After 2-day post-eclosion, flies with the respective genotypes were transferred to new longevity vials with a density of 30 flies per vial. Numbers of dead flies were counted daily. Fresh food vial was provided and replaced every 2 days during the assay. At least 60 flies per genotype were used in the assay.

Rapid Iterative Negative Geotaxis Assay

We used the rapid iterative negative geotaxis (RING) assay to determine glioma fly climbing ability (locomotor activity) [24]. Control flies (*UAS-hCD4-tdGFP*; *repo-GAL4, tub-GAL80^{ts}*) have an average climbing height of ~4–5 cm in a 3-s time period. Flies that remain at the bottom are assigned to a value of 0. In brief, 30 flies are transferred to clean polystyrene vials and rest for 20 min before testing. A digital camera is used to document negative geotaxis by scoring the height that flies climbed within 10 s. Index 1 represents for 0 to 2.5 cm, 2 for 2.5 to 5.0 cm, 3 for 5.0 to 7.5, and 4 for 7.5 to 10 cm in 10 s. Higher score represents better climbing ability. It is critical not to reuse the polystyrene testing vials in this assay after the initial sets of data are gathered because new flies placed into used vials will not climb to the same extent as in fresh vials.

Olfactory Associative Memory Assays

All the flies were kept at 19 °C until eclosion and then shifted to 30 °C for 4 days before training to avoid the *tub-GAL80^{ts}* inhibition. The 3-min and 3-h memory assays were also performed at 30 °C. Groups of approximately 50–100 flies were exposed first to one odor (the conditioned stimulus, CS+; 3-octanol or 4-methyl-cyclohexanol) paired with 12 × 1.5-s pulses of 75-V DC electric shock presented at 5-s interpulse intervals. This was followed by the presentation of a second odor (CS–; 4-methyl-cyclohexanol or 3-octanol) without electric shock. In the testing phase, the flies were presented with a choice between CS+ and CS– odors in a T-maze for 2 min. At the end of this 2-min period, the flies trapped in each T-maze arm were anesthetized and counted. From the distribution of flies between the two arms, the performance index (PI) was calculated as the number of flies avoiding the shocked odor

(CS+) minus the number avoiding the non-shocked odor (CS–), divided by the total number of flies and multiplied by 100.

Human Glioma Cell Lines and Culture Conditions

Human glioma cell lines U-87 MG and U-118 MG were maintained in Dulbecco's modified Eagle's medium (DMEM) supplemented with 10% fetal bovine serum (FBS), penicillin, and streptomycin in a humidified atmosphere of 5% CO₂, 95% air at 37 °C. LN-229 and GBM8401 cells were cultured in DMEM supplemented with 5% FBS, penicillin, and streptomycin in a humidified atmosphere of 5% CO₂, 95% air at 37 °C.

RNA Isolation and Quantitative Real-time PCR

The procedures of total mRNA extraction, cDNA synthesis, and quantitative RT-PCR were following previous protocol [25]. The normal brain cDNA was purchased from OriGene Technologies Inc. (Rockville, MD, USA). The reverse transcripts were amplified and quantified using an Illumina ECO™ Real-Time PCR system. The relative quantitative gene expression was normalized to GAPDH as an internal control and then calculated using the 2^{-ΔΔC_t} method. The qPCR primer pairs used were as follows: ACAT1 forward 5'-GCTC GTGTTCTGGTCCTATGTG-3' and reverse 5'-TAGA ACATCCTGTCACCAAAGCG-3'; GAPDH forward 5'-CTTCATTGACCTCAACTAC-3' and reverse 5'-GCCA TCCACAGTCTTCTG-3'.

Cell Lysate Preparation and Western Blot

Cultured cells were lysed by RIPA buffer (100 mM Tris-HCl, 150 mM NaCl, 0.1% SDS, and 1% Triton X-100) at 4 °C for 10 min, and the cell lysates were harvested by centrifugation at 15,000 rpm for 10 min to obtain the supernatants. The normal brain lysates were purchased from Abcam. The Western blotting was performed as described in [26]. Thirty-microgram cell lysates from each group were applied to 10% sodium dodecyl sulfate polyacrylamide gel electrophoresis, and proteins were transferred onto polyvinylidene difluoride membranes (Bio-Rad Laboratories, Inc.). The membrane was blocked with 5% skim milk in TBST for 1 h at room temperature. The primary antibodies used include specific for ACAT1 (Santa Cruz Biotechnology) and β-actin (Santa Cruz Biotechnology). Band detection was conducted by enhanced chemiluminescence and X-ray film (GE Healthcare, Piscataway, NJ, USA).

Immunohistochemistry

Tissue microarray (TMA) is recognized as a scientific tool to evaluate tumors by histological and immunohistochemical methods. In this study, 44 cases of various grades of gliomas

and 10 cases of non-neoplastic brain tissue were collected. TMA slides constructed from paraffin-embedded tumor tissues were obtained from the Department of Pathology, Tri-Service General Hospital. The initial tissue section processes, including the procedure of dewax, rehydrate, and antigen retrieval, were performed according to previous protocol [27]. After then, sections of TMA were incubated with a mouse monoclonal ACAT1 antibody (Santa Cruz Biotechnology) (1:200 diluted in phosphate-buffered saline (PBS); Spring Bioscience, Pleasanton, CA, USA) for 1 h at room temperature. After washed three times (each for 5 min in PBS), TMA sections were incubated with biotin-labeled secondary immunoglobulin (1:100, DAKO, Glostrup, Denmark) for 1 h at room temperature. The following step was applying 3-amino-9-ethylcarbazole substrate chromogen (DAKO) at room temperature to visualize peroxidase activity after three washes by PBS. Finally, TMA slides were mounted and imaged.

Fly Brain Volume Measurement

In this study, seven adult brains from each group were imaged and processed with Imaris software (Bitplane). To measure the brain in 3D, we loaded z-stack fluorescent images (membrane GFP-labeled glia cells) generated from confocal microscopy (Zeiss LSM880) into the Imaris software. We then used “create surface” tool to make a solid surface of the entire adult brain. During this process, we followed the *surface creation wizard* and adjusted intensity thresholding to yield a solid surface best matching brain morphology. Next, all the statistics data, including volume, can be exported for further analysis.

Cell Viability Assay

Glioma cells were harvested and seeded in multiple 96-well plates at 1×10^3 cells/well in 100- μ l growth medium with or without K-604 treatment (Sigma SML 1837). Cells were then incubated for 72 h before viability assay using MTS Cell Proliferation Assay Kit (BioVision). Twenty-microliter MTS solution containing PES was added to each well and incubated for 2 h at 37 °C in a humidified, 5% CO₂ incubator. The assay was performed by using an ELISA reader at 490 nm to establish baseline readings.

Statistics

Log-rank test for survival analysis and all results are expressed as mean values \pm SEM. Student's *t* test or one-way analysis of variance was used for comparisons between groups. A *p* value < 0.05 was considered to be statistically significant differences. Patient survival data was automatically calculated by Project Betastasis using a log-rank test. Heat map was generated in R language (version 3.2.3).

Results

Pathometabolic Gene Expression Associated with Reduced Patient Survival in GBM

In high-grade gliomas, glucose, glutamine, and lipid metabolic pathways are considerably reprogrammed [6]. We reason that evolutionarily conserved metabolic genes such as many carbohydrate and lipid metabolic genes might also regulate gliomagenesis. To investigate this, we started looking into the 739 evolutionarily conserved candidate genes that were possibly essential to glial function and were discovered from the glial-specific RNAi screen [16]. We used the Project Betastasis online tool to perform an in silico analysis of the survival probabilities of these candidate genes from the REMBRANDT glioma database (<http://betastasis.com/glioma/rembrandt/>) as described previously [23]. We first divided all tumor samples from the REMBRANDT dataset into low- and high-expressing groups based on the gene profiling results. Kaplan–Meier survival curves revealed that the high-expressing group comprising *ALDOA*, *ACAT1*, *ELOVL6*, and *LOX* significantly correlated with poor survival in patients with high-grade gliomas (*p* < 0.001 in all four candidate genes) (Fig. 1). Moreover, these results are in agreement with those obtained from an online integrated system, PRECOG (*P*REdiction of *C*linical *O*utcomes from *G*enomic Profiles; <https://precog.stanford.edu/>) (Fig. S1). Among these genes, *ALDOA* (Aldolase/CG6058 in fly) is responsible for glycolysis in the cell, *ACAT1* (CG8112 in fly) and *ELOVL6* (Baldspot/CG3971 in fly) participates in cellular lipid metabolism, and *LOX* (Lox/CG11335 in fly) encodes a secreted protein whose extracellular role is to promote tumor invasion in vivo in both *Drosophila* and mammalian glioma models [28]. The strategy of considering the genes essential to glial function (obtained from the in vivo RNAi screen) in combination with the results of the bioinformatics analysis of gliomas in patients might provide a new rationale for identification of potential biomarkers.

Generation of a Novel Adult *Drosophila* Glioma Model

To validate the aforementioned pathometabolic genes in an animal model, we aimed to generate a new *Drosophila* model to recapitulate the phenotypes of survival and neurobehavior seen in adult patients with glioblastoma. We modified the previous EGFR-PI3K larval model [17] by introducing a temporal expression system (Fig. 2a) [22]. In this system, the temperature sensitive mutant GAL80^{ts} prevented EGFR and PI3K expression driven by a glia-specific GAL4 (*repo-GAL4*) when cultured at 19 °C, and the suppression effect allowed the animal to survive through the entire developmental stages and reach adulthood. Shifting the incubation temperature from 19 to 30 °C repressed GAL80 functioning and induced EGFR-

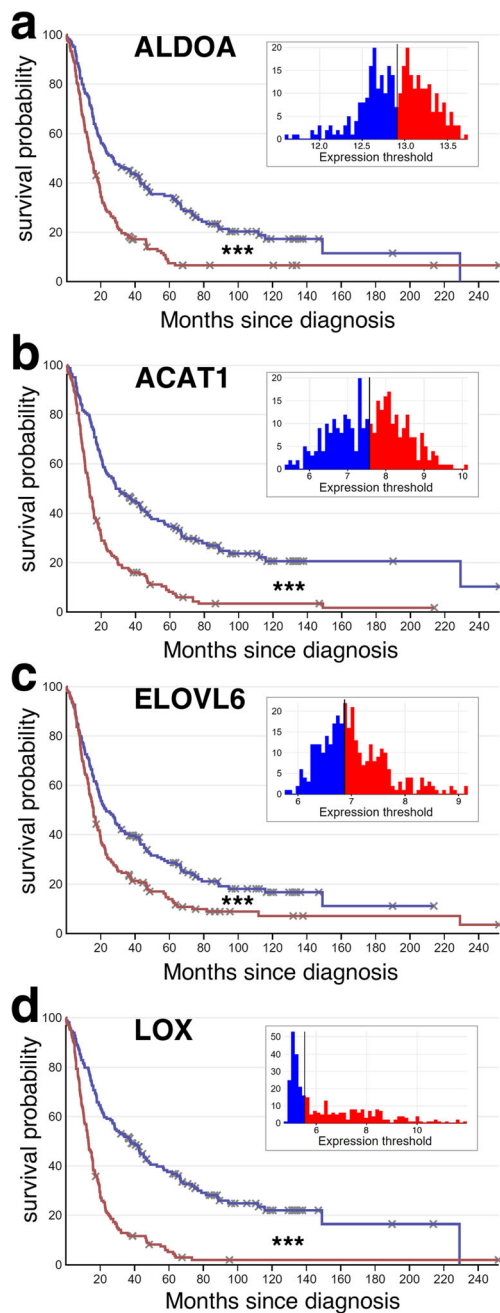


Fig. 1 Candidate metabolic genes were identified as associated with poor patient survival in high-grade gliomas. The Kaplan–Meier survival curve analysis of glioma patient survival data according to high (red) and low (blue) mRNA expression of **a** *ALDOA*, **b** *ACAT1*, **c** *ELOVL6*, and **d** *LOX*, obtained from REMBRANDT transcriptomic data (total 523 glioma patients). Patients were stratified by high and low gene expression thresholding at the median value. The cutoff point is shown in the histogram of insets (Project Betastasis online representation tool, <http://www.betastasis.com>). Asterisks show significance levels (log-rank test, $***p < 0.001$)

PI3K signaling in adult glial cells. Comparison of the brain size of animals exposed to different heat shock durations (Figs. 2b and 4c) revealed that, consistent with the larval glioma model, CNS enlargement and dramatic glial overgrowth also occurred

in the adult glioma flies. After 8 days of heat shock treatment, the volume of the adult glioma brain was almost two times larger than the control (Fig. 4a, control $1.31 \times 10^7 \pm 0.071 \text{ m}^3$; glioma $2.24 \times 10^7 \pm 0.223 \text{ m}^3$). Flow cytometric analysis also showed a mark increase of glia cell population (from 14.2 to 60.2%) among total brain cells (Fig. S2).

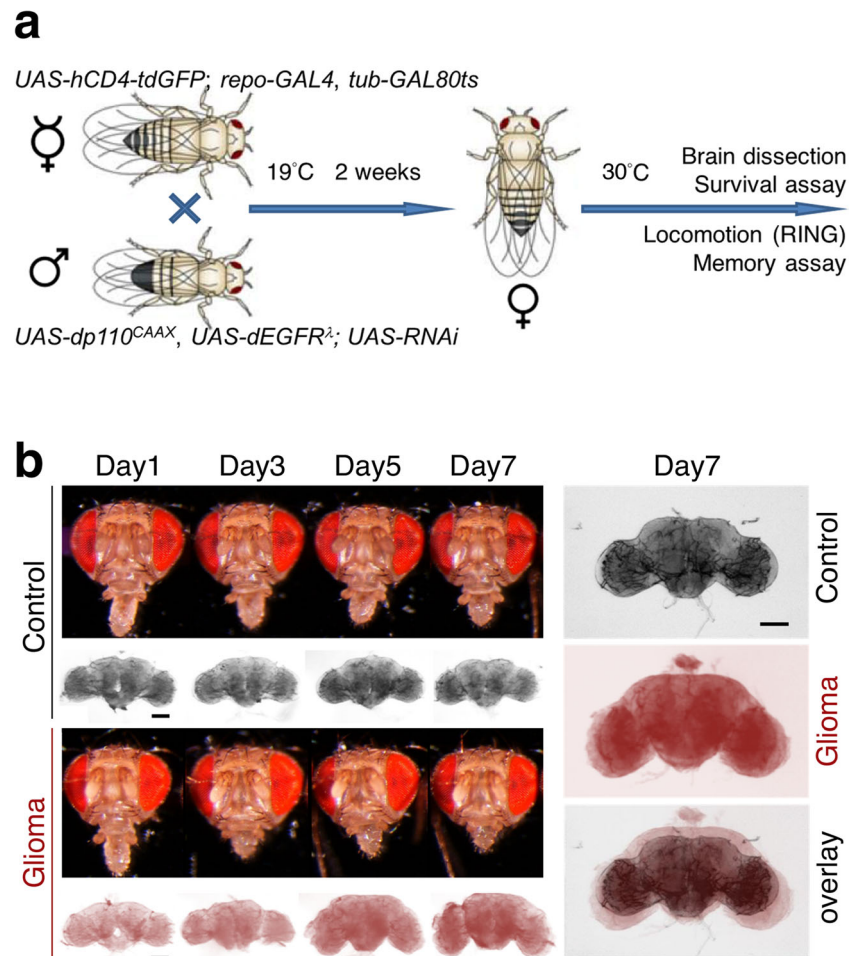
Adult Glioma Fly Has Shorter Lifespan and Defective Neural Behaviors

After 5–7 days of exposure to a temperature of 30 °C, we observed that adult glioma flies frequently exhibited some extent of motor deficit, followed by death. Adult glioma flies also exhibited a much shorter lifespan than control flies (Fig. 3a, median survival time of control group 28.5 days; glioma group 8.1 days). Results of the rapid iterative negative geotaxis (RING) assay showed that the climbing ability reduced in a time-dependent manner during glioma progression (Fig. 3b). A progressive decline in neuropsychological functioning was also observed in high-grade glioma patients [29]. To examine whether the adult glioma model is able to recapitulate neurocognitive dysfunction in glioma patients, we performed olfactory associative memory assays by using glioma animal with 3–4 days of heat shock treatment [30]. In this stage, flies still have regular brain size and exhibit no detectable locomotion defects. Flies from the glioma group showed a marked decline in memory at 3 h after conditioning, but this effect was not seen 3 min after conditioning (Fig. 3c), indicating a significant memory defect. Taken together, this adult glioma model presents several phenotypic features that resemble the patients' symptoms, including brain tumor enlargement, shorter lifespan, and cognitive impairments.

In Vivo Identification of Pathometabolic Pathways in GBM

Larval glioma model had been used for kinome-wide genetic screen for new genes involved in glioma development [18]. We then tried to assess whether our adult glioma model is also suitable for genetic screening. We first performed experiments using conditional RNAi constructs targeting key members in the signaling pathway that had been reported to be essential for gliomagenesis. Our primary focus was assessing adult survival, because of the complex nature of animal death and the sizable sample number. The three key pathways we verified are as follows: (1) tumor proliferation–related pathway (E2F1, [31]), (2) tumor migration pathway (WNK1/OSR1/NKCC1 pathway, [32]), (3) EGFR/RTK signaling pathway. Since these three pathways are required for glial pathogenesis, we expected a suppressor phenotype (i.e., longer lifespan) when there was a reduced candidate gene expression by RNAi in the glioma background. As anticipated, RNAi targeting E2F1 and NCC69 (human NKCC1 orthologue) extended the median

Fig. 2 An adult *Drosophila* model for human glioma. **a** Scheme of generation of adult *Drosophila* glioma model. **b** Coactivation of EGFR and PI3K in adult glia induces marked brain enlargement after heat shock for days (30 °C). External morphology of adult heads (top panels) has no obvious change after days of heat shock treatment. Dissected adult brains (bottom panel) of control flies exhibit normal brain size after 7 days heat shock (30 °C). Glioma flies have normal brain size on day 1. Gradually enlarged brains were observed when glioma flies were heat shocked during adult stage (days 3–7). The right panel image marked “overlay” represents a superimposition of two images of control (gray) and glioma (red) brains after 7 days heat shock for demonstrating the enlargement of glioma brain. Scale bar = 100 μ m



survival time to 14 and 11 days, respectively (8.1 days in glioma animals). EGFR RNAi knockdown animals showed 100% survival rate when the heat shock treatment was stopped after 3 weeks (Fig. S3). This indicated that the survival of adult glioma flies can be modified by different pathogenic features of gliomagenesis. This adult glioma model can also be used as a genetic screening platform for identifying new oncogenic candidates in GBM.

We next examined whether the four pathometabolic genes identified by bioinformatics approaches could be validated in vivo by using the adult fly glioma model. In the longevity assay, the lifespan of pathometabolic gene knockdown animals was extended by 2 to 4 days compared to that of glioma flies after EGFR-PI3K coinduction (Fig. 4a). These results are consistent with the TCGA and REMBRANDT glioma datasets. Patients with low expression of pathometabolic genes have better survival after diagnosis (Fig. 1). Among these four genes, we were particularly interested in *ACATI* because of its role in regulating ER-cholesterol homeostasis and lipid metabolism. *ACATI* converts cholesterol to cholesterol esters for storage as lipid droplets and subsequently modulates lipid metabolism [33, 34]. Recent studies indicated that cholesterol homeostasis is linked to human diseases, such as

hypertension and atherosclerosis. Moreover, *ACATI* is highly expressed in many different cancer types, but still little is known about its role in human glioma.

To rule out the off-target effect of the specific RNAi used, two additional RNAi lines targeting a different *ACATI* gene coding region were further examined, and, similar to previous results, a prolonged lifespan was observed in the adult glioma model (Fig. 4b). Both bioinformatics analysis of patient samples and longevity assays in flies demonstrated that the *ACATI* gene plays a crucial role in adult glioma survival. Since *ACATI* knockdown suppresses the glioma-induced short lifespan, it might also reduce the brain enlargement associated with gliomas. We then analyzed brain volume by confocal imaging. 3D rendered brain images and volume measurements showed that *ACATI* knockdown in glia resulted in reduced brain size on the eighth day of heat shock treatment (Fig. 4c, d). Interestingly, *ACATI* knockdown during development also caused marked reduction of larval glioma in the CNS (Fig. S4). Lowering the gene expression of *ACATI* greatly suppressed glioma brain enlargement in both larval and adult models, but, nevertheless, the glioma-bearing animals still died much earlier. These observations collectively indicate that some

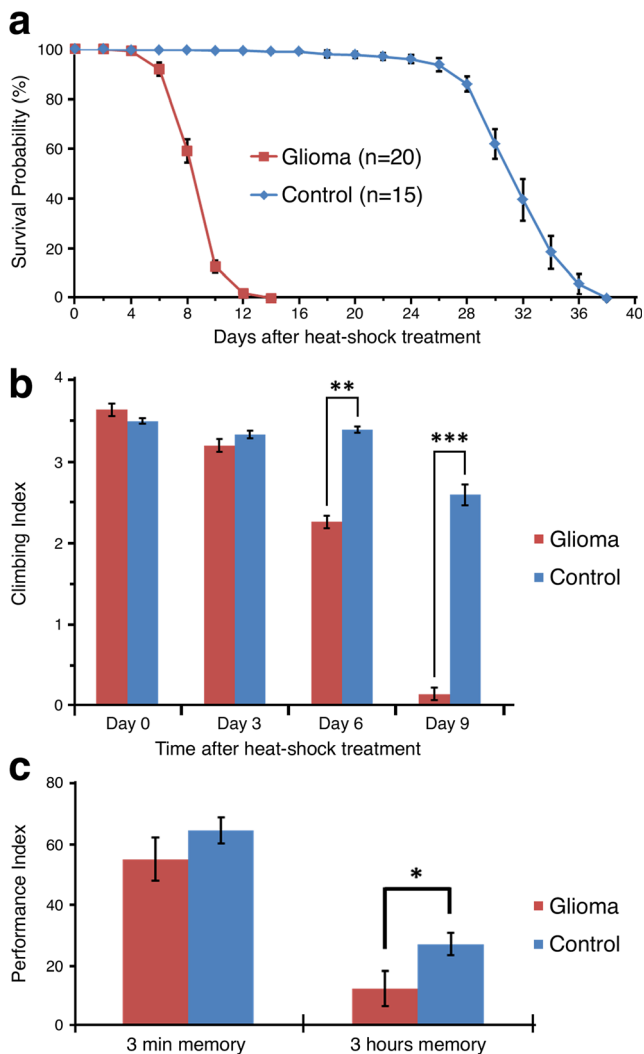


Fig. 3 Adult glioma flies exhibit short lifespan, locomotor defects, and memory deficits. **a** Longevity was assessed in *Drosophila* by counting living flies every 2 days over time. The median survival time of adult glioma flies is about 8.1 days. In control group, it is approximately 31 days. Each survival data is obtained from 30 female flies in a food vial. Each group contains more than 15 independent vials (*n*). **b** Glioma flies show early locomotor defect. In the rapid iterative negative geotaxis (RING) assay, higher score represents better climbing ability. Experimental details can be found in “Materials and Methods.” Locomotor activity of glioma flies starts to decline at day 6 after glioma induction. Each group contains *n* = 6 vials (30 flies per vial) and significance is indicated as stars (*) relative to the control group with $^{**}p < 0.01$ and $^{***}p < 0.001$. **c** Olfactory associative memory assay of 4-day heat shock flies revealed that glioma group exhibited defects of 3-h olfactory aversive associative memory as compared to the control groups ($^{*}p < 0.05$; ANOVA followed by Tukey’s test, *n* = 8, 13, 9, 10 from left to right bars)

important brain functions, other than glia overproliferation, are significantly compromised during tumorigenesis and ultimately lead to glioma-related death. Taken together, our novel adult fly glioma model identified a key cholesterol metabolic enzyme *ACAT1*, which regulates EGFR-PI3K-dependent gliomagenesis in vivo.

High Expression of ACAT1 in GBM Cell Lines and High-Grade Glioma Samples

To relate *Drosophila* data with human GBM cell lines and patients, we first examined *ACAT1* mRNA and protein expression in GBM cell lines. We found that both *ACAT1* mRNA and protein were expressed and significantly upregulated in all four glioma cell lines, especially in U-118 MG (Fig. 5a, b). Based on the available gene expression/mutation information for the cell lines from ATCC and the integrated database *canSAR* (<https://cansar.icr.ac.uk/>), only U-118 MG cells show both high levels of EGFR expression and PTEN mutation among the four cell lines tested (U-87 MG: EGFR^{low}, PTEN^{mt}; LN-229: EGFR^{high}, PTEN^{wt}; GBM8401: unknown). This correlation might suggest the involvement of a possible EGFR-PI3K-dependent *ACAT1* up-regulation mechanism.

Additionally, compared to that in normal brain tissues and WHO grade I–II gliomas, *ACAT1* showed higher expression in WHO grade III–IV gliomas (Fig. 5c). The reported results for human tissue specimens were similar to those for GBM cell lines and *Drosophila*. Therefore, our in vitro and in vivo data support the hypothesis that *ACAT1* might be a potential prognostic factor for human gliomas.

Blocking ACAT1 Activity Suppresses GBM Cell Viability

Knockdown of *ACAT1* expression markedly suppressed glioma development in the adult fly model. However, it is unclear whether the *ACAT1* protein itself or its enzymatic activity for cholesterol esterification is crucial for tumorigenesis. To examine tumor cell growth, a potent and selective *ACAT1* inhibitor, K-604, was applied to glioma cells. Unlike the commonly used *ACAT* inhibitor, avasimibe, which is known to inhibit both *ACAT1* and *ACAT2* [35], K-604 shows a much higher specificity for *ACAT1* than for *ACAT2* (IC₅₀ values for human *ACAT1* 0.45 μmol/l; *ACAT2* 102.85 μmol/l [36]). *ACAT1* inhibition was found to suppress glioma cell viability (Fig. 5d), supporting that *ACAT1* is an oncotarget for human gliomas. It is worth noting that U-118 MG is relatively resistant to K-604, and this resistance is correlated to high *ACAT1* expression (Fig. 5a, b). This phenomenon also suggests a cell context-dependent involvement on drug resistance. Together, these in vitro data show that GBM cells are sensitive to blockade of *ACAT1* enzymatic function on cholesterol esterification.

Discussion

In recent years, metabolic reprogramming in GBM has been extensively studied in an attempt to demystify pathways involved in cancer cell metabolism [37]. Earlier, cancer cells

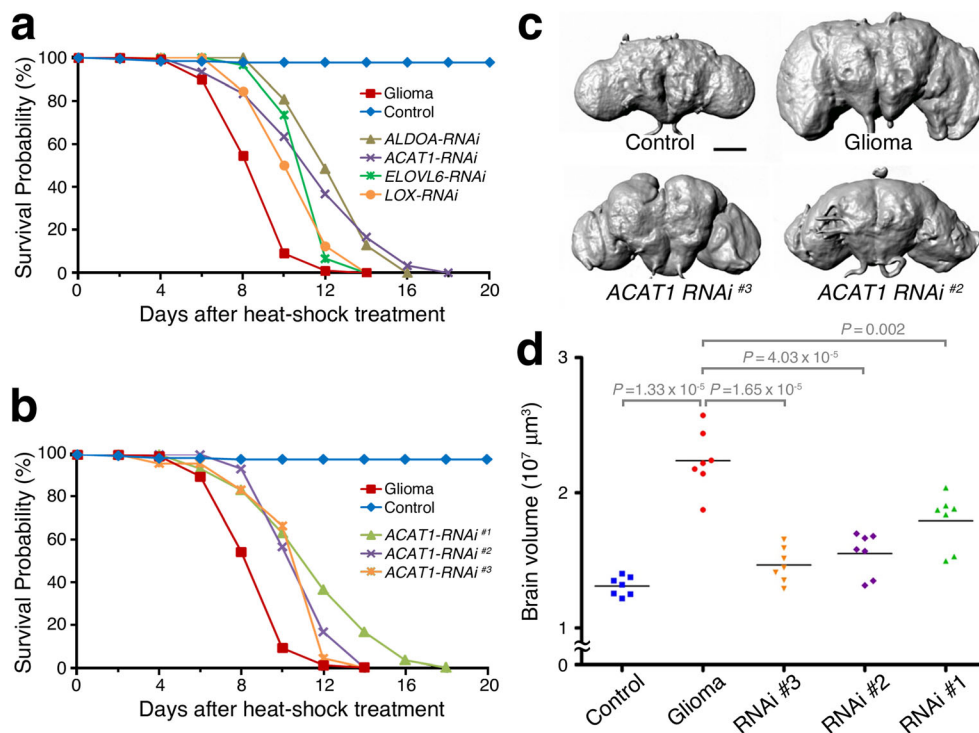


Fig. 4 Knockdown pathometabolic gene expression partly relieve glioma-induced phenotypes in *Drosophila*. **a** Glial-specific knockdown of *ALDOA*, *ACAT1*, *ELOVL6*, and *LOX* extends lifespan of glioma flies. Each group contains 30 flies. **b** *ACAT1* knockdown by using different RNAi exhibits a consistent prolonged lifespan in glioma flies: RNAi #1 (8112R-2 from NIG-FLY); RNAi #2 (110347 from VDRC); RNAi #3

(#63035 from BDSC). Each group contains 30 flies. **c** The confocal 3D rendered brain images showed a marked reduction of brain size when knockdown *ACAT1* expression in glioma background. 100 μm scale bars. **d** The quantitation of 3D brain volume of control, GBM, and three *ACAT1* RNAi transgenic flies. The adjusted *p* value was calibrated between each group ($n = 7$ for each group)

were thought to utilize only glucose for energy metabolism; however, recent findings suggest that they also use fatty acids and amino acids. Thus, the Warburg effect is being overruled by novel concepts. Bioenergetic signal transduction pathways such as AMP-activated protein kinase (AMPK) and mammalian target of rapamycin (mTOR) signaling are linked to oncogenic signaling within glioma cells. These pathways contribute to metabolic stress and promote cell cycle progression and metabolic flexibility, thereby increasing GBM cell survival [38, 39]. Here, we demonstrated that *ALDOA* (glycolysis), *ACAT1* and *ELOVL6* (lipogenesis), and *LOX* drive GBM pathogenesis. *ACAT1* plays a key role in cellular lipid metabolism [33], which is located in the endoplasmic reticulum and synthesizing cholesterol esters for lipid droplet formation [34]. Recent studies have shown that *ACAT1* is expressed in cancers of the breast [40], kidneys [41], and pancreas [42]. Our and others' [43] data showed that *ACAT1/SOAT1* is overexpressed in human high-grade gliomas and inhibition of *ACAT1* suppressed glioma cell growth. These results support our hypothesis that metabolic genes are involved in glioma development.

The metabolic difference between normal cells and GBM cells may provide new therapeutic strategies. At present, bioinformatics application has provided a robust and useful tool

to study human diseases. Online databases such as Project Betastasis, the Gene Expression Omnibus (GEO), and PREdiction of Clinical Outcomes from Genomic profiles (PRECOG) were established for investigating the correlations between cancer outcomes and genomic profiles [23, 44, 45]. Using these platforms for large-scale genome-wide screening of glioma patient survival, we found that *ALDOA*, *ACAT1*, *ELOVL6*, and *LOX* expression correlates with poor survival in high-grade gliomas.

Owing to the major limitation of using glioma cell line models is the lack of in vivo tumor microenvironments, in vivo glioma models such as development of transgenic or xenograft-based orthotopic glioma murine models are considered worthwhile. Nevertheless, those are not only time-consuming but also costly. The in vivo larval *Drosophila* glioma model is generated by coactivation of EGFR-Ras and PI3K during embryogenesis in glial progenitor cells, which causes neoplasia that recapitulates many key features of human glioma with regard to increased proliferation, migration, and invasiveness [17]. Moreover, this approach is also useful for identifying new targets involved in GBM development [18]. However, the potential limitation of the larval *Drosophila* glioma system is that early activation of the gliomagenic

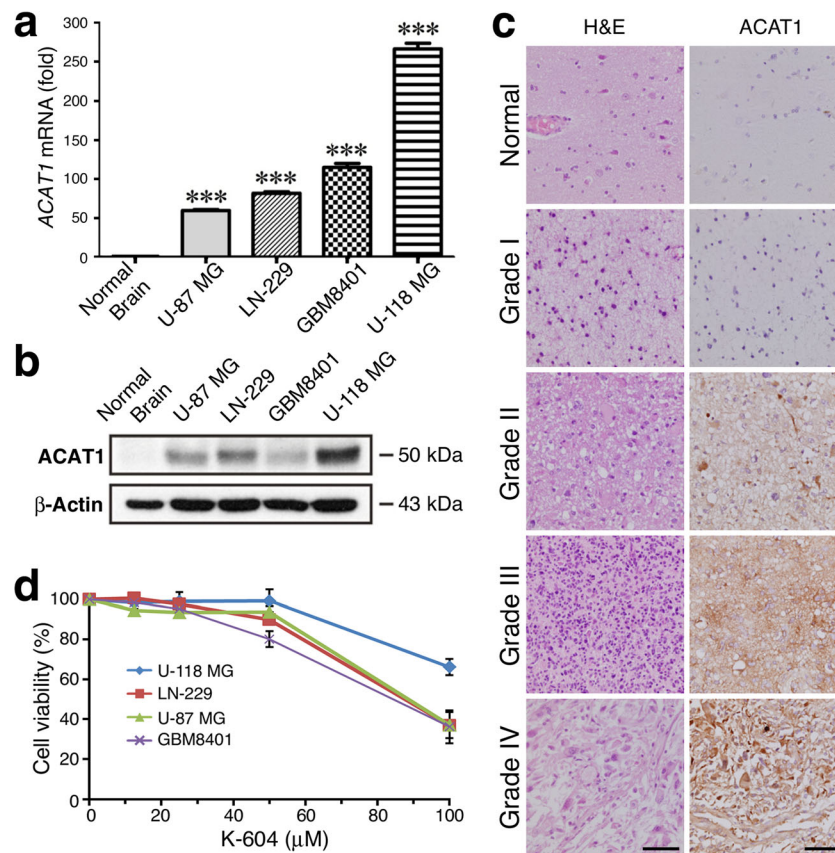


Fig. 5 High expression of ACAT1 in GBM cell lines and patient samples. **a** *ACAT1* mRNA expression obtained by using real-time RT-PCR in four different GBM cell lines. The relative expressions were normalized with normal brain tissue. Bars, mean values \pm SEM, *** $p < 0.001$ showed significant differences. Data are representative of three independent experiments. **b** ACAT1 protein level analyzed by Western blot. **c** IHC staining showed higher intensity and percentage expression of ACAT1 in high-grade gliomas than in low-grade gliomas and non-tumor part of brain tissues. Representative hematoxylin and eosin (H&E) staining and

immunohistochemical staining of ACAT1 of normal brain, grade I pilocytic astrocytomas, grade II diffuse astrocytomas, grade III anaplastic astrocytomas, and grade IV glioblastomas. Original magnification $\times 400$. **d** Blocking ACAT1 activity by K-604 suppresses GBM viability. Human glioma cells were treated by K-604 with different concentrations (0, 12.5, 25, 50, and 100 μM) for 72 h, and then, cell viability was measured using the MTS assay. Error bars represent the standard deviation derived from three independent experiments

signaling pathway causes larval mortality; therefore, it is not feasible to study neurobehavioral problems in human adulthood. In contrast, our model introduces a temporal expression system. This model better mimics human gliomas by allowing us to investigate survival and neural behavior of adult glioma flies. Moreover, we were not only able to observe brain tumor enlargement in adult flies, which is similar to human glioma in adulthood, but also manage the initiation of gliomagenesis. Therefore, our adult *Drosophila* glioma model overcomes the developmental bias associated with the larval model and therefore is more useful to study survival in glioma patients. This in vivo adult *Drosophila* model system provides several robust phenotypic readouts, including brain volume, glial cell number, locomotion, survival, and other high-function behavioral paradigms such as olfactory associative memory, which allow us to decipher pathogenic signaling pathways in a whole-animal setting.

Intriguingly, echoing our current finding on *ELOVL6*, a recent review article also pointed out that *ELOVL6* is overexpressed in GBM patients and correlates with reduced patient survival [46]. Our adult fly glioma model showed the first in vivo evidence regarding *ELOVL6*'s involvement in gliomagenesis. Moreover, an *ELOVL6* inhibitor, compound A [47], was discovered and had been showed to interfere with tumor growth in lung squamous cell carcinoma in vivo [48]. It will be valuable to develop a drug screening platform by using our model system to test low-molecular-weight compounds, such as K-604, TMZ, vitamin E, and compound A, on treating adult fly glioma. Taken together, our approach involving bioinformatics analysis and screening of candidate genes using our adult *Drosophila* glioma model, followed by validation using human glioma cell models and brain tumor tissues provides a promising way to study glioma.

Acknowledgments We thank Henry Sun for providing critical reagents; Yi-Hsin Pan for performing flow cytometric assays, FlyCore in Taiwan for providing reagents, and Instrument Center of National Defense Medical Center for confocal imaging facility.

Funding Information This study was supported by grants from Health and Welfare surcharge of tobacco to the Ministry of Health and Welfare (MOHW106-TDU-B-211-144001 to D.-Y.H.), Ministry of Science and Technology (MOST-104-2745-B-007-002 and MOST-106-2314-B-016-012-MY3 to D.-Y.H.; MOST-105-2628-B-001-011-MY3 to T.-Y.L.; MOST-107-3017-F-007-004), Tri-Service General Hospital (TSGH-C106-004-006-008-S04 to D.-Y.H.), and Ministry of National Defense-Medical Affairs Bureau (MAB-106-019 to D.-Y.H. and MAB-106-121 to T.-Y.L.), Taipei, Taiwan, R.O.C.

References

- Stupp R, Mason WP, van den Bent MJ, Weller M, Fisher B, Taphoorn MJ, Belanger K, Brandes AA et al (2005) Radiotherapy plus concomitant and adjuvant temozolomide for glioblastoma. *N Engl J Med* 352(10):987–996. <https://doi.org/10.1056/NEJMoa043330>
- Ostrom QT, Gittleman H, Farah P, Ondracek A, Chen Y, Wolinsky Y, Stroup NE, Kruchko C et al (2013) CBTRUS statistical report: primary brain and central nervous system tumors diagnosed in the United States in 2006–2010. *Neuro-Oncology* 15(Suppl 2):ii1–i56. <https://doi.org/10.1093/neuonc/not151>
- Lenting K, Verhaak R, Ter Laan M, Wesseling P, Leenders W (2017) Glioma: experimental models and reality. *Acta Neuropathol* 133(2):263–282. <https://doi.org/10.1007/s00401-017-1671-4>
- Kegelman TP, Hu B, Emdad L, Das SK, Sarkar D, Fisher PB (2014) In vivo modeling of malignant glioma: the road to effective therapy. *Adv Cancer Res* 121:261–330. <https://doi.org/10.1016/B978-0-12-800249-0.00007-X>
- Warburg O (1956) On respiratory impairment in cancer cells. *Science* 124(3215):269–270
- Wolf A, Agnihotri S, Guha A (2010) Targeting metabolic remodeling in glioblastoma multiforme. *Oncotarget* 1(7):552–562. <https://doi.org/10.18632/oncotarget.101014>
- Grassian AR, Coloff JL, Brugge JS (2011) Extracellular matrix regulation of metabolism and implications for tumorigenesis. *Cold Spring Harb Symp Quant Biol* 76:313–324. <https://doi.org/10.1101/sqb.2011.76.010967>
- Seyfried TN, Flores R, Poff AM, D'Agostino DP, Mukherjee P (2015) Metabolic therapy: a new paradigm for managing malignant brain cancer. *Cancer Lett* 356(2 Pt A):289–300. <https://doi.org/10.1016/j.canlet.2014.07.015>
- Madhavan S, Zenklusen JC, Kotliarov Y, Sahni H, Fine HA, Buetow K (2009) Rembrandt: helping personalized medicine become a reality through integrative translational research. *Mol Cancer Res* 7(2):157–167. <https://doi.org/10.1158/1541-7786.MCR-08-0435>
- Brennan CW, Verhaak RG, McKenna A, Campos B, Nounshmehr H, Salama SR, Zheng S, Chakravarty D et al (2013) The somatic genomic landscape of glioblastoma. *Cell* 155(2):462–477. <https://doi.org/10.1016/j.cell.2013.09.034>
- Cancer Genome Atlas Research N (2008) Comprehensive genomic characterization defines human glioblastoma genes and core pathways. *Nature* 455(7216):1061–1068. <https://doi.org/10.1038/nature07385>
- Masui K, Cavenee WK, Mischel PS (2016) Cancer metabolism as a central driving force of glioma pathogenesis. *Brain Tumor Pathol* 33(3):161–168. <https://doi.org/10.1007/s10014-016-0265-5>
- Ru P, Williams TM, Chakravarti A, Guo D (2013) Tumor metabolism of malignant gliomas. *Cancers* 5(4):1469–1484. <https://doi.org/10.3390/cancers5041469>
- Lee Y, Morrison BM, Li Y, Lengacher S, Farah MH, Hoffman PN, Liu Y, Tsingalia A et al (2012) Oligodendroglia metabolically support axons and contribute to neurodegeneration. *Nature* 487(7408):443–448. <https://doi.org/10.1038/nature11314>
- Funfschilling U, Supplie LM, Mahad D, Boretius S, Saab AS, Edgar J, Brinkmann BG, Kassmann CM et al (2012) Glycolytic oligodendrocytes maintain myelin and long-term axonal integrity. *Nature* 485(7399):517–521. <https://doi.org/10.1038/nature11007>
- Ghosh A, Kling T, Snaidero N, Sampaio JL, Shevchenko A, Gras H, Geurten B, Gopfert MC et al (2013) A global in vivo Drosophila RNAi screen identifies a key role of ceramide phosphoethanolamine for glial ensheathment of axons. *PLoS Genet* 9(12):e1003980. <https://doi.org/10.1371/journal.pgen.1003980>
- Read RD, Cavenee WK, Furnari FB, Thomas JB (2009) A drosophila model for EGFR-Ras and PI3K-dependent human glioma. *PLoS Genet* 5(2):e1000374. <https://doi.org/10.1371/journal.pgen.1000374>
- Read RD, Fenton TR, Gomez GG, Wykosky J, Vandenberg SR, Babic I, Iwanami A, Yang H et al (2013) A kinome-wide RNAi screen in Drosophila Glia reveals that the RIO kinases mediate cell proliferation and survival through TORC2-Akt signaling in glioblastoma. *PLoS Genet* 9(2):e1003253. <https://doi.org/10.1371/journal.pgen.1003253>
- Agnihotri S, Golbourn B, Huang X, Remke M, Younger S, Cairns RA, Chalil A, Smith CA et al (2016) PINK1 is a negative regulator of growth and the Warburg effect in glioblastoma. *Cancer Res* 76(16):4708–4719. <https://doi.org/10.1158/0008-5472.CAN-15-3079>
- Cheng P, Wang J, Waghmare I, Sartini S, Coviello V, Zhang Z, Kim SH, Mohyeldin A et al (2016) FOXD1-ALDH1A3 signaling is a determinant for the self-renewal and tumorigenicity of mesenchymal glioma stem cells. *Cancer Res* 76(24):7219–7230. <https://doi.org/10.1158/0008-5472.CAN-15-2860>
- Chen L, Zhang Y, Yang J, Hagan JP, Li M (2013) Vertebrate animal models of glioma: understanding the mechanisms and developing new therapies. *Biochim Biophys Acta* 1836(1):158–165. <https://doi.org/10.1016/j.bbcan.2013.04.003>
- McGuire SE, Le PT, Osborn AJ, Matsumoto K, Davis RL (2003) Spatiotemporal rescue of memory dysfunction in Drosophila. *Science* 302(5651):1765–1768. <https://doi.org/10.1126/science.1089035>
- Bourgonje AM, Verrijp K, Schepens JT, Navis AC, Piepers JA, Palmén CB, van den Eijnden M, Hooft van Huijsdijnen R et al (2016) Comprehensive protein tyrosine phosphatase mRNA profiling identifies new regulators in the progression of glioma. *Acta Neuropathol Commun* 4(1):96. <https://doi.org/10.1186/s40478-016-0372-x>
- Gargano JW, Martin I, Bhandari P, Grotewiel MS (2005) Rapid iterative negative geotaxis (RING): a new method for assessing age-related locomotor decline in Drosophila. *Exp Gerontol* 40(5):386–395. <https://doi.org/10.1016/j.exger.2005.02.005>
- Feng SW, Chen Y, Tsai WC, Chiou HC, Wu ST, Huang LC, Lin C, Hsieh CC et al (2016) Overexpression of Telo2 decreases survival in human high-grade gliomas. *Oncotarget* 7(29):46056–46066. <https://doi.org/10.18632/oncotarget.10021>
- Hueng DY, Tsai WC, Chiou HY, Feng SW, Lin C, Li YF, Huang LC, Lin MH (2015) DDX3X biomarker correlates with poor survival in human gliomas. *Int J Mol Sci* 16(7):15578–15591. <https://doi.org/10.3390/ijms160715578>
- Tsai WC, Hueng DY, Lin CK (2015) Nuclear overexpression of urocorin discriminates primary brain tumors from reactive gliosis. *APMIS* 123(6):465–472. <https://doi.org/10.1111/apm.12374>
- Kim SN, Jeibmann A, Halama K, Witte HT, Walte M, Matzat T, Schillers H, Faber C et al (2014) ECM stiffness regulates glial

- migration in *Drosophila* and mammalian glioma models. *Development* 141(16):3233–3242. <https://doi.org/10.1242/dev.106039>
29. Sizoo EM, Braam L, Postma TJ, Pasman HR, Heimans JJ, Klein M, Reijneveld JC, Taphoorn MJ (2010) Symptoms and problems in the end-of-life phase of high-grade glioma patients. *Neuro-Oncology* 12(11):1162–1166. <https://doi.org/10.1093/neuonc/nop045>
 30. Wu CL, Chang CC, Wu JK, Chiang MH, Yang CH, Chiang HC (2018) Mushroom body glycolysis is required for olfactory memory in *Drosophila*. *Neurobiol Learn Mem* 150:13–19. <https://doi.org/10.1016/j.nlm.2018.02.015>
 31. Alonso MM, Alemany R, Fueyo J, Gomez-Manzano C (2008) E2F1 in gliomas: a paradigm of oncogene addiction. *Cancer Lett* 263(2):157–163. <https://doi.org/10.1016/j.canlet.2008.02.001>
 32. Zhu W, Begum G, Pointer K, Clark PA, Yang SS, Lin SH, Kahle KT, Kuo JS et al (2014) WNK1-OSR1 kinase-mediated phosphorylation of Na⁺-K⁺-2Cl⁻ cotransporter facilitates glioma migration. *Mol Cancer* 13:31. <https://doi.org/10.1186/1476-4598-13-31>
 33. Chang TY, Li BL, Chang CC, Urano Y (2009) Acyl-coenzyme A: cholesterol acyltransferases. *Am J Phys Endocrinol Metab* 297(1):E1–E9. <https://doi.org/10.1152/ajpendo.90926.2008>
 34. Hashemi HF, Goodman JM (2015) The life cycle of lipid droplets. *Curr Opin Cell Biol* 33:119–124. <https://doi.org/10.1016/j.ceb.2015.02.002>
 35. Llaverias G, Laguna JC, Alegret M (2003) Pharmacology of the ACAT inhibitor avasimibe (CI-1011). *Cardiovasc Drug Rev* 21(1):33–50
 36. Ikenoya M, Yoshinaka Y, Kobayashi H, Kawamine K, Shibuya K, Sato F, Sawanobori K, Watanabe T et al (2007) A selective ACAT-1 inhibitor, K-604, suppresses fatty streak lesions in fat-fed hamsters without affecting plasma cholesterol levels. *Atherosclerosis* 191(2):290–297. <https://doi.org/10.1016/j.atherosclerosis.2006.05.048>
 37. Agnihotri S, Zadeh G (2016) Metabolic reprogramming in glioblastoma: the influence of cancer metabolism on epigenetics and unanswered questions. *Neuro-Oncology* 18(2):160–172. <https://doi.org/10.1093/neuonc/nov125>
 38. Masui K, Tanaka K, Akhavan D, Babic I, Gini B, Matsutani T, Iwanami A, Liu F et al (2013) mTOR complex 2 controls glycolytic metabolism in glioblastoma through FoxO acetylation and upregulation of c-Myc. *Cell Metab* 18(5):726–739. <https://doi.org/10.1016/j.cmet.2013.09.013>
 39. Vucicevic L, Misirkic M, Janjetovic K, Vilimanovich U, Sudar E, Isenovic E, Prica M, Harhaji-Trajkovic L et al (2011) Compound C induces protective autophagy in cancer cells through AMPK inhibition-independent blockade of Akt/mTOR pathway. *Autophagy* 7(1):40–50
 40. Antalis CJ, Arnold T, Rasool T, Lee B, Buhman KK, Siddiqui RA (2010) High ACAT1 expression in estrogen receptor negative basal-like breast cancer cells is associated with LDL-induced proliferation. *Breast Cancer Res Treat* 122(3):661–670. <https://doi.org/10.1007/s10549-009-0594-8>
 41. Sbiera S, Leich E, Liebisch G, Sbiera I, Schirbel A, Wiemer L, Matysik S, Eckhardt C et al (2015) Mitotane inhibits sterol-O-acyl transferase 1 triggering lipid-mediated endoplasmic reticulum stress and apoptosis in adrenocortical carcinoma cells. *Endocrinology* 156(11):3895–3908. <https://doi.org/10.1210/en.2015-1367>
 42. Li J, Gu D, Lee SS, Song B, Bandyopadhyay S, Chen S, Konieczny SF, Ratliff TL et al (2016) Abrogating cholesterol esterification suppresses growth and metastasis of pancreatic cancer. *Oncogene* 35(50):6378–6388. <https://doi.org/10.1038/onc.2016.168>
 43. Geng F, Cheng X, Wu X, Yoo JY, Cheng C, Guo JY, Mo X, Ru P et al (2016) Inhibition of SOAT1 suppresses glioblastoma growth via blocking SREBP-1-mediated lipogenesis. *Clin Cancer Res* 22(21):5337–5348. <https://doi.org/10.1158/1078-0432.CCR-15-2923>
 44. Gentles AJ, Newman AM, Liu CL, Bratman SV, Feng W, Kim D, Nair VS, Xu Y et al (2015) The prognostic landscape of genes and infiltrating immune cells across human cancers. *Nat Med* 21(8):938–945. <https://doi.org/10.1038/nm.3909>
 45. Cheng YP, Lin C, Lin PY, Cheng CY, Ma HI, Chen CM, Hueng DY (2014) Midkine expression in high grade gliomas: correlation of this novel marker with proliferation and survival in human gliomas. *Surg Neurol Int* 5:78. <https://doi.org/10.4103/2152-7806.133205>
 46. Shergalis A, Bankhead A 3rd, Luesakul U, Muangsin N, Neamati N (2018) Current challenges and opportunities in treating glioblastoma. *Pharmacol Rev* 70(3):412–445. <https://doi.org/10.1124/pr.117.014944>
 47. Shimamura K, Kitazawa H, Miyamoto Y, Kanesaka M, Nagumo A, Yoshimoto R, Aragane K, Morita N et al (2009) 5,5-Dimethyl-3-(5-methyl-3-oxo-2-phenyl-2,3-dihydro-1H-pyrazol-4-yl)-1-phenyl-3-(trifluoromethyl)-3,5,6,7-tetrahydro-1H-indole-2,4-dione, a potent inhibitor for mammalian elongase of long-chain fatty acids family 6: examination of its potential utility as a pharmacological tool. *J Pharmacol Exp Ther* 330(1):249–256. <https://doi.org/10.1124/jpet.109.150854>
 48. Marien E, Meister M, Muley T, Gomez Del Pulgar T, Derua R, Spraggins JM, Van de Plas R, Vanderhoydonc F et al (2016) Phospholipid profiling identifies acyl chain elongation as a ubiquitous trait and potential target for the treatment of lung squamous cell carcinoma. *Oncotarget* 7(11):12582–12597. <https://doi.org/10.18632/oncotarget.7179>